



HAL
open science

Heme Uptake in *Lactobacillus sakei* Evidenced by a New Energy Coupling Factor (ECF)-Like Transport System

Emilie Verplaetse, Gwenaëlle André-Leroux, Philippe Duhutrel, Gwendoline Coeuret, Stéphane Chaillou, Christina Nielsen-Leroux, Marie-Christine Champomier-Vergès

► To cite this version:

Emilie Verplaetse, Gwenaëlle André-Leroux, Philippe Duhutrel, Gwendoline Coeuret, Stéphane Chaillou, et al.. Heme Uptake in *Lactobacillus sakei* Evidenced by a New Energy Coupling Factor (ECF)-Like Transport System. *Applied and Environmental Microbiology*, 2020, 86 (18), pp.1-41. 10.1128/AEM.02847-19 . hal-02939244

HAL Id: hal-02939244

<https://hal.inrae.fr/hal-02939244v1>

Submitted on 15 Sep 2020

HAL is a multi-disciplinary open access archive for the deposit and dissemination of scientific research documents, whether they are published or not. The documents may come from teaching and research institutions in France or abroad, or from public or private research centers.

L'archive ouverte pluridisciplinaire **HAL**, est destinée au dépôt et à la diffusion de documents scientifiques de niveau recherche, publiés ou non, émanant des établissements d'enseignement et de recherche français ou étrangers, des laboratoires publics ou privés.

1 **Title:** Heme uptake in *Lactobacillus sakei* evidenced by a new ECF-like transport system.

2

3 Emilie Verplaetse¹, Gwenaëlle André-Leroux², Philippe Duhutrel^{1,3}, Gwendoline Coeuret¹,

4 Stéphane Chaillou¹, Christina Nielsen-Leroux¹, Marie-Christine Champomier-Vergès^{1*}

5 1) Université Paris-Saclay, INRAE, AgroParisTech, Micalis Institute, 78350, Jouy-en-
6 Josas, France.

7 2) Université Paris-Saclay, INRAE, MaIAGE, 78350, Jouy-en-Josas, France.

8 3) Present address: bioMérieux, 5 rue des Aqueducs, 69290 Craponne, France.

9

10

11

12

13 Running title: heme transport in *Lactobacillus sakei*

14

15 *Corresponding author: marie-christine.champomier-verges@inrae.fr

16

17 Key-words: iron, lactic acid bacteria, ABC-transporter

18

19 **Abstract**

20 *Lactobacillus sakei* is a non-pathogenic lactic acid bacterium and a natural inhabitant of meat
21 ecosystems. Although red meat is a heme-rich environment, *L. sakei* does not need iron or
22 heme for growth, while possessing a heme-dependent catalase. Iron incorporation into *L. sakei*
23 from myoglobin and hemoglobin was formerly shown by microscopy and the *L. sakei* genome
24 reveals the complete equipment for iron and heme transport. Here, we report the
25 characterization of a five-gene cluster (*lsa1836-1840*) encoding a putative metal iron ABC
26 transporter. Interestingly, this cluster, together with a heme dependent catalase gene, is also
27 conserved in other species from the meat ecosystem. Our bioinformatic analyses revealed that
28 the locus might correspond to a complete machinery of an Energy Coupling Factor (ECF)
29 transport system. We quantified *in vitro* the intracellular heme in wild-type (WT) and in our
30 Δ *lsa1836-1840* deletion mutant using an intracellular heme sensor and ICP-Mass spectrometry
31 for quantifying incorporated ^{57}Fe heme. We showed that in the WT *L. sakei*, heme
32 accumulation occurs rapidly and massively in the presence of hemin, while the deletion mutant
33 was impaired in heme uptake; this ability was restored by *in trans* complementation. Our
34 results establish the main role of the *L. sakei* Lsa1836-1840 ECF-like system in heme uptake.
35 Therefore, this research outcome sheds new light on other possible functions of ECF-like
36 systems.

37

38

39 **Importance**

40 *Lactobacillus sakei* is a non-pathogenic bacterial species exhibiting high fitness in heme rich
41 environments such as meat products, although it does not need iron nor heme for growth.
42 Heme capture and utilization capacities are often associated with pathogenic species and are
43 considered as virulence-associated factors in the infected hosts. For these reasons, iron

44 acquisition systems have been deeply studied in such species, while for non-pathogenic
45 bacteria the information is scarce. Genomic data revealed that several putative iron transporters
46 are present in the genome of the lactic acid bacterium *L. sakei*. In this study, we demonstrate
47 that one of them, is an ECF-like ABC transporter with a functional role in heme transport. Such
48 evidence has not yet been brought for an ECF, therefore our study reveals a new class of heme
49 transport system.

50

51

52 **Introduction**

53

54 Iron is an essential element for almost all living organisms (1) and heme, an iron-containing
55 porphyrin, is both a cofactor of key cellular enzymes and an iron source for bacteria. Many
56 bacteria encode the complete heme biosynthesis pathway to be autonomous for heme
57 production and partly to guarantee their iron supply. However, some others lack heme
58 biosynthetic enzymes and rely on the environment to fulfill their heme requirements.

59 *Lactococcus lactis* and all known *Lactobacilli* are heme-auxotrophic bacteria (2). Also, it is
60 well established that lactic acid bacteria do not require iron to grow (3) and that their growth is
61 unaffected by iron deprivation. Nevertheless, numerous lactic acid bacteria, such as *L. lactis*,
62 *Lactobacillus plantarum*, or *Enterococcus faecalis*, require exogenous heme to activate
63 respiration growth in the presence of heme (2).

64 *Lactobacillus sakei* is a non-pathogenic lactic acid bacterium frequently found on fresh meat. *L.*
65 *sakei* is systematically associated with meat products and in particular with raw meat products
66 stored at low temperature and under vacuum packaging (4). Interestingly, abundance of *L.*
67 *sakei* has been shown to prevent growth of undesirable pathogens such as *Listeria*
68 *monocytogenes* (5, 6), *Escherichia coli* O157:H7 in both cooked and minced meat (5, 7, 8), and
69 of spoilers such as *Brochothrix thermosfacta* (7, 8). Therefore, this species is often used as a
70 bioprotective culture in meat products. Nevertheless, mechanisms of synergy and competition
71 between species in such complex matrices are still poorly understood (9). Meat, can be
72 considered as a growth medium naturally rich in iron and heme. Quantification of total iron
73 content in raw meat reported a mean of 2.09 mg total iron/100 g for four beef meat cuts in
74 which 87% was heme iron (10). Although *L. sakei* has a tropism for meat and is known to
75 possess a heme-dependent catalase (11), it is considered to be a bacterium that requires neither
76 iron nor heme to grow (12).

77 First insights on iron/heme utilization by *L. sakei* came from its whole genome analysis (13)
78 with the identification of coding sequences of several iron transporters, regulators and iron-
79 containing enzymes. Later, microscopy analysis of *L. sakei* cells combined to spectroscopy
80 methods showed that *L. sakei* is able to incorporate iron atoms from complexed iron such as
81 myoglobin, hemoglobin, hematin, and transferrin (12). This suggested that *L. sakei* may display
82 heme or hemic-iron storage ability, although the analytical method used was not quantitative
83 and the precise amount of iron compound that *L. sakei* is able to store was not determined.
84 Hematin did not show any effect on growth of *L. sakei*, but hematin has been shown to prolong
85 bacteria viability in stationary phase (13). However, the mechanisms underlining *L. sakei*
86 survival in the presence of heme need to be unraveled.

87 Heme acquisition systems have mainly been studied in Gram-negative and Gram-positive
88 pathogens that acquire heme from host hemoproteins in a two steps process (for a review, see
89 (14–16)). First, cell surface or secreted proteins scavenge free heme molecules or complexed
90 heme. Then, transmembrane transporters, generally ATP-binding cassette (ABC) transporters,
91 carry the heme moiety into the intracellular space. Gram-positive bacteria rely mainly on
92 surface-exposed receptors that shuttle heme through the cell-wall and deliver it to an ABC
93 transporter for subsequent transfer into the cytoplasm. Within Gram-positive pathogens, one of
94 the most well characterized heme uptake system is the *Staphylococcus aureus* Iron Surface
95 Determinants (Isd) system. The staphylococcal machinery is inserted into a ten-gene locus
96 encoding cell-wall anchored proteins (IsdABCH), a membrane transport system (IsdDEF), a
97 sortase (SrtB) and two cytoplasmic heme-oxygenases (IsdG and IsdI) (17, 18). IsdB and IsdH
98 are responsible for binding host hemoproteins or heme. IsdA extracts heme from IsdB or IsdH
99 and transfers it to IsdC. Funneled heme is finally transferred into the cytoplasm through the
100 membrane by the IsdDEF ABC transporter where it is finally degraded to release free iron by
101 the heme oxygenases IsdG and IsdI. Several of these Isd proteins contain *Near* iron Transporter

102 (NEAT) domain, present only in Gram-positive bacteria, and specific to interact with
103 hemoproteins and heme. NEAT domain is a 150-acid residues domain that despite sequence
104 variability displays a conserved β -barrel and a hydrophobic pocket involved in heme binding
105 (19).

106 Thus far, heme acquisition systems in heme auxotrophic organisms have only been reported for
107 *Streptococci* (15, 20, 21). In *S. pyogenes*, the system involves the Shr and Shp NEAT-domain
108 proteins and the Hts ABC transporter (20, 22, 23). In *Lactococcus lactis*, heme homeostasis,
109 especially heme efflux systems, have been deeply characterized (24, 25). Nevertheless, the
110 acquisition of exogenous heme remains poorly characterized. Heme transport across *L. sakei*
111 membrane is still unknown. Additionally, bioinformatic analysis shows that the genome of *L.*
112 *sakei* does not contain any NEAT domain (13) which suggests that heme transit could involve
113 transport systems distinct from *Streptococci* and *S. aureus* (14).

114 Regarding prokaryotic metal ion uptake transporters, comparative and functional genomic
115 analysis have identified Energy-Coupling Factor (ECF) transporters as a novel type of ABC
116 importers widespread in Gram-positive bacteria and first identified in lactic acid bacteria (26).
117 The studies identified genes encoding a ABC-ATPases plus three or four membrane proteins
118 within the same or adjacent to operons, which were implicated in vitamin production or
119 synthesis of metal-containing metalloenzymes (27). Their predicted role in cobalt or nickel ions
120 uptake and delivery within the cell was demonstrated in *Salmonella enterica* and *Rhodoccus*
121 *capsulatus*, respectively. Since then, ECF-coding genes have been evidenced in *Mycoplasma*,
122 *Ureaplasma* and *Streptococcus* strains. They were also shown to function as importers not only
123 for transition metal ions but also for vitamins as riboflavin and thiamine (27). Recently, several
124 ECF systems have been characterized, among them folate and pantothenate ECF transport in
125 *Lactobacillus brevis*, and cobalt ECF in *R. capsulatus* (28–31). It was evidenced that ECF
126 transporters constitute a novel family of conserved membrane transporters in prokaryotes,

127 while sharing a similar four domains organization as the ABC transporters. Each ECF displays
128 a pair of cytosolic nucleotide-binding ATPases (the A and A' components also called EcfA and
129 EcfA'), a membrane-embedded substrate-binding protein (the S component or the EcfS), and a
130 transmembrane energy-coupling component (The T component or EcfT). The quadripartite
131 organization has a 1:1:1:1 stoichiometry. Notably, the S component renders ECF
132 mechanistically distinct from ABC transport systems as it is predicted to shuttle within the
133 membrane, when carrying the bound substrate from the extracellular side into the cytosol (see
134 the recent review (26)). Accordingly, the S-component solely confers substrate specificity to
135 the uptake system (28). Till the 2000s, folate, riboflavin and thiamine ECF importers have been
136 reported for *L. lactis* (32–34). Similarly, folate, hydroxyl pyrimidine and pantothenate ECFs
137 have been reported and structurally characterized for *L. brevis* (28, 30, 31), both Gram-positive
138 rod shape species of lactic acid bacteria.

139 In this paper, we mainly targeted *L. sakei* locus *lsa1836-1840* encoding a putative ABC
140 transporter, and demonstrated its role as a heme uptake system, combining *in silico*
141 bioinformatics analysis with *in vitro* functional analysis. We showed that this system encodes
142 the complete machinery of an ECF-like importer, including the extracellular proteins that
143 initiate heme scavenging. In parallel, we quantified the heme-and heminic iron storage
144 properties of *L. sakei*, and compared WT *L. sakei* with the Δ *lsa1836-1840* *L. sakei* deletion and
145 overexpression mutants using an intracellular heme-reporter gene and mass-spectrometry
146 quantification of iron-labelled heme. We were able to show *in vitro* that this five-gene locus
147 plays an important role in active heme import.

148

149 **Results**

150

151 **1. Putative iron and heme transport systems in *Lactobacillus sakei***

152 Accurate analysis of the genome of *L. sakei* 23K (13), focused on heme/iron transport systems
153 and heme utilization enzymes, previously led to the identification of six putative iron/heme
154 transport systems and one heme-degrading enzyme (Table 1). First, two genes *lsa0246* and
155 *lsa1699* encoding proton motive permeases, which belong to the MntH family of manganese
156 uptake, might be involved in iron or heme uptake. Notably, in *L. lactis*, a *mntH* mutant was
157 impaired in Fe²⁺ transport (35).

158 Second, an operon, composed of the genes *lsa1194-1195* coding for poorly defined membrane
159 proteins of the CCC1 family, is putatively involved in iron transport. In yeast, CCC1 is
160 involved in the manganese and iron ions transport from the cytosol to the vacuole for storage
161 (36).

162 Third, two ABC systems homologous to the HrtAB and Pef heme-detoxification systems
163 present in *L. lactis* and *Streptococcus agalactiae* (24, 37) were also identified in *L. sakei*
164 genome. These systems are encoded by the *lsa1366-1367* and *lsa0419-0420* genes,
165 respectively. The sequencing of the *lsa0419-0420* region has confirmed the presence of a
166 frameshift and indicated that these genes are not expressed in *L. sakei* 23K strain. The *lsa1366-*
167 *1367* gene products are homologous to the *L. lactis* *Llmg_0625-0624* encoded proteins. The *L.*
168 *lactis* genes code for the HrtB and HrtA proteins, respectively (24). An *in silico* analysis of
169 *Lsa1367* and HrtB indicated that these proteins share 33% of sequence identity and,
170 accordingly, the same fold, as assessed by TOPPRED analysis (38). Particularly, the
171 cytoplasmic-exposed Y168 and Y231 amino-acid residues, shown as important for HrtB-heme
172 interaction in *L. lactis* (25), are also present in *Lsa1367*, which suggests that these genes might
173 be homologous to the *L. lactis* heme export system.

174 Last, two iron or heme uptake ABC-transporters were identified. Markedly, the operon
175 *lsa0399-0402* encodes a Fhu system, sharing homology with various orthologous genes and
176 operons encoding complexed iron transport systems, and possibly homologous to the *Listeria*

177 *monocytogenes* HupCGD system. Also, *L. monocytogenes* shows that HupCGD and Fhu are
178 involved in heme and ferrioxamine uptake, respectively (39).
179 Then, the ABC system encoded within *lsa1836-1840* genes was automatically annotated as
180 involved in cobalamin transport, whilst it shows some levels of similarities with heme import
181 systems described in Gram-positive bacteria (40–43). At first, we carried out a multiple
182 alignment of all putative substrate-binding lipoproteins encoded in the *L. sakei* 23K genome
183 and noticed that Lsa1839 protein was closely related to Lsa0399 from the Fhu system (data not
184 shown), suggesting a possible link to iron/heme transport. Furthermore, if heme transportation
185 would represent a specific fitness for growth in meat, we wondered whether other meat-borne
186 bacteria would contain a similar cluster in their genome. As shown in Figure 1, comparative
187 genomic analysis revealed that the *lsa1836-1840* genes cluster is present in several species
188 known to harbor a tropism for meat. The most interesting observation is that species harboring
189 the *lsa1836-1840*-like cluster also have in their genome a *katA* gene, encoding a heme
190 dependent catalase, while the other species lacking the cluster, such
191 as *Leuconostoc* and *Lactococcus*, were shown to be deprived of catalase-encoding gene.
192 Although such co-occurrence could not constitute a proof of the role of the *lsa1836-1840*
193 cluster in heme transport, this analysis provided an additional argument consolidating this
194 hypothesis.

195

196 **2. The *lsa1836-1840* encodes an ECF like transport system putatively involved in heme** 197 **transport**

198 Due to the conservation of the operon *lsa1836-1840*, each of the five sequences was analyzed
199 comprehensively using bioinformatics. It includes multiple sequence alignment, as well as 3D
200 structure, proteins network and export peptide predictions. Lsa1836 shows a sequence
201 similarity of more than 30%, associated to a probability above 99% with an e-value of $8 \cdot e^{-15}$, to

202 share structural homology with the membrane-embedded substrate-binding protein component
203 S from an ECF transporter of the closely related *L. brevis*, as computed by HHpred (44).
204 Accordingly, its sequence is predicted to be an integral membrane component with six
205 transmembrane helices, and a very high rate of hydrophobic and apolar residues, notably 11
206 tryptophan amino-acid residues among the 230 residues of the full-length protein (Fig. 2A).
207 HHpred analysis indicates that Lsa1837 shares more than 50 % sequence similarity with the
208 ATPase subunits A and A' of the same ECF in *L. brevis* (Fig. 2A). With 100% of probability
209 and a e-value of $1. e^{-35}$, Lsa1837 describes two repetitive domains, positioned at 9-247 and 299-
210 531, where each refers structurally to one ATPase very close in topology to the solved ATPase
211 subunits, A and A' of ECF from *L. brevis*, respectively. Appropriately, the N-terminal and C-
212 terminal ATPases, are predicted to contain an ATP-binding site. Lsa1837 could correspond to
213 the fusion of ATPase subunits, A and A'. Protein Lsa1838 shows sequence similarity of above
214 30%, with a probability of 100 % and e-value of $1. e^{-30}$, to share structural homology with the
215 membrane-embedded substrate-binding protein component T from the ECF transporter of *L.*
216 *brevis* (Fig. 2A). Interestingly, similar bioinformatic analysis of sequence and structure
217 prediction demonstrates that Lsa1839 and Lsa1840 share both 99.8% structural homology, and
218 e-value of $1. e^{-24}$ and of $1. e^{-21}$, with the β and α domains of human transcobalamin, respectively
219 (Fig. 2A). Consistently, both proteins have an export signal located at their N-terminal end.
220 Taken together, these results predict with high confidence that the transcriptional unit encodes
221 the complete machinery of an ECF, including the extracellular proteins that initiate the
222 scavenging of iron-containing heme (Fig. 2A). Each protein compartment is predicted through
223 the presence/absence of its signal peptide as being extracellular, embedded in the membrane or
224 cytosolic. Correspondingly, every protein sequence associates appropriate subcellular location
225 with respect to its predicted function. In line with that, the network computed by String for the
226 set of proteins of the operon shows that they interact together from a central connection related

227 to Lsa1837, which corresponds to the ATP-motor couple of ATPases (45). The transcriptional
228 unit also encompasses Lsa1839 and Lsa1840, highly homologous to β and α subunits of
229 transcobalamin respectively, that are highly hypothesized to initiate the scavenging of heme
230 from the extracellular medium. To address the capacity of those subunits of transcobalamin-
231 like binding domain to bind a heme moiety, we homology-modeled Lsa1839 and Lsa1840. We
232 then assembled the biological unit composed of the heterodimer formed by β and α subunits,
233 using the related 3D templates of corresponding subunit of haptocorrin and transcobalamin.
234 Subsequently, an iron-containing heme moiety was docked into the groove, located at the
235 interface of the complex formed by the two proteins. The docking highlights a heme-binding
236 through polar and hydrophobic interactions. Nevertheless, no particular π stacking could be
237 detected (Fig. 2B). The redocking of cobalamin in haptocorrin and cyanocobalamin in
238 transcobalamin shows a binding energy of -17 and -12 kcal/mol, respectively (Fig. 2B). With a
239 binding energy of -9 kcal/mol, the heme bound to the crevice formed by Lsa1839 and Lsa1840
240 displays an affinity in the same range than the endogenous ligands, and emphasizes that the
241 assembly composed of Lsa1839 and Lsa1840 could be compatible with the recognition and
242 binding of a heme (Fig. 2B). To resume, Lsa1836-1840 describes a complete machinery that
243 could be able to internalize a heme instead or additionally to a cobalamin molecule.
244 Importantly, this operon includes also the extracellular scavenging α - and β -like subunits of
245 transcobalamin, which promotes the S-component Lsa1836 as likely very specific for iron-
246 containing heme. Markedly, the S-component displays a closely conserved fold, yet it does not
247 show any of the strictly conserved residues known to bind specifically cobalt-containing
248 cobalamin.

249 No heme synthesis enzymes are present in *L. sakei* genome, nevertheless a gene coding for a
250 putative heme-degrading enzyme of the Dyp-type peroxidase family, *lsa1831*, was identified in
251 the *L. sakei* genome (Table 1). Its structure is predicted to be close to DypB from *Rhodococcus*

252 *jostii* (46). Interestingly, residues of DypB involved in the porphyrin-binding, namely Asp153,
253 His226 and Asn246, are strictly conserved in Lsa1831 (47). Markedly, the *lsa1831* gene is
254 located upstream of the *lsa1836-1840* operon putatively involved in the active heme transport
255 across the membrane.

256 Our bioinformatical analysis allows the functional reannotation of the *lsa1836-1840* genes into
257 the complete machinery of an Energy-Coupling Factor, possibly dedicated to the transport of
258 iron through the heme (Fig. 3A-B). Consistently, the Lsa1831 enzyme, which is close to the
259 *lsa1836-1840* loci, could participate downstream to release iron from the heme once inside the
260 cytoplasm.

261

262 **3. The Lsa1836-1840 is *in vitro* an effective actor of heme uptake in *L. sakei*.**

263 To confirm the above transporter as involved in heme trafficking across the membrane, a
264 *lsa1836-1840* deletion mutant was constructed by homologous recombination. The *L. sakei*
265 Δ *lsa1836-1840* mutant was analyzed for its capacity to internalize heme using an intracellular
266 heme sensor developed by Lechardeur and co-workers (24). This molecular tool consists in a
267 multicopy plasmid harboring a transcriptional fusion between the heme-inducible promoter of
268 *hrtR*, the *hrtR* coding sequence and the *lacZ* reporter gene, the pP_{hrt} *hrtR-lac* (Table 2). In *L.*
269 *lactis*, HrtR is a transcriptional regulator that represses the expression of a heme export system,
270 HrtA and HrtB, as well as its own expression in the absence of heme. Upon heme binding, the
271 repression is alleviated allowing the expression of the export proteins (24). As *L. sakei*
272 possesses the *lacLM* genes, it was necessary to construct the Δ *lsa1836-1840* mutant in the *L.*
273 *sakei* RV2002 strain, a *L. sakei* 23K Δ *lacLM* derivative, yielding the RV4057 strain (Table 2).
274 The pP_{hrt} *hrtR-lac* was then introduced in the RV2002 and RV4057 strains, yielding the
275 RV2002 *hrtR-lac* and the RV4057 *hrtR-lac* strains (Table 2). β -Galactosidase (β -Gal) activity
276 of the RV4057 *hrtR-lac* strain, grown in a chemically defined medium (MCD) (48) in the

277 presence of 0.5, 1 and 5 μM hemin, was determined and compared to that of the RV2002 *hrtR-*
278 *lac* used as control (Fig. 4A). We showed that hemin reached the intracellular compartment as
279 β -Gal expression was induced by hemin. Relative β -Gal activity of the RV4057 *hrtR-lac*
280 mutant strain showed a slight increase as compared to the WT at 0.5 μM heme but a
281 statistically significant two-fold reduction was measured at 1 μM heme and further, a 40%
282 reduced activity was shown at higher hemin concentration. This indicates that the intracellular
283 abundance of heme is significantly reduced in the RV4057 bacterial cells at 1 and 5 μM heme,
284 while it is similar to the WT at low heme concentrations. The method described above did not
285 allow us to quantify the absolute amount of heme incorporated by bacteria as only cytosolic
286 heme may interact with HrtR. Therefore, we used hemin labeled with the rare ^{57}Fe isotope
287 (^{57}Fe -Hemin) combined with Inductively Coupled Plasma Mass Spectrometry (ICP-MS) to
288 measure with accuracy the total hemic-iron content of cells. Quantification of ^{57}Fe was used
289 as a proxy to quantify heme. The absolute number of heme molecules incorporated by the
290 $\Delta\textit{lsa1836-1840}$ mutant was also quantified using ^{57}Fe -hemin. The $\Delta\textit{lsa1836-1840}$ mutant was
291 constructed in the WT *L. sakei* 23K genetic background to obtain the RV4056 strain (Table 2).
292 Bacteria were incubated in the MCD, in the absence or in the presence of 1, 5 or 40 μM of ^{57}Fe -
293 hemin. ICP-MS quantification indicated that the ^{57}Fe content of the two strains was similar at 1
294 μM ^{57}Fe -hemin. By comparison with the WT, a 5-fold reduction in the ^{57}Fe content of the
295 RV4056 strain at 5 μM heme concentration and a 8-fold reduction at 40 μM heme were
296 measured (Fig. 4B).

297 To confirm the major role of the *lsa1836-1840* gene products in heme acquisition, we analyzed
298 the ^{57}Fe content of the RV4056 strain harboring the *pPlsa1836-1840*, a multicopy plasmid that
299 expresses the *lsa1836-1840* operon under its own promoter, and compared it to the WT. The
300 quantification of the ^{57}Fe atoms in the RV4056 *pPlsa1836-1840* bacteria shows a 1.3 time and a

301 7 times higher iron content at 5 and 40 μM ^{57}Fe -hemin, respectively, by comparison with
302 measurements done on WT bacteria (Fig. 4C).

303 These experiments confirm that the Lsa1836-1840 system is involved *in vitro* in the active
304 incorporation of heme in *L. sakei*.

305

306 **4. Heme accumulates inside the *L. sakei* cytosol at low heme concentrations**

307 We then addressed the ability for *L. sakei* to consume heme or iron to survive. We knew from a
308 previous study that *L. sakei* incorporates preferentially heminic-compounds from the medium,
309 probably as an adaptation to its meat environment (12). Data obtained previously showed that
310 the incorporation of heme molecules are qualitatively correlated with both the concentration of
311 heme in the growth medium, and the survival properties of the bacteria in stationary phase,
312 suggesting that *L. sakei* could use heme or iron for its survival (See Supplemental text, Fig. S1
313 and S2). Nevertheless, heme incorporation could not be quantified with accuracy in the
314 previous studies. To tackle that, the intracellular heme levels incorporated by *L. sakei* were
315 quantified. The RV2002 *hrtR-lac* strain (Table 2) was grown in MCD in the presence of
316 increasing concentration of hemin, and the β -Gal activity of cells was measured (Fig. 5A). We
317 showed that the β -Gal activity increased with the concentration of the hemin molecule in the
318 growth medium. A plateau was reached when cells were grown in 0.75 - 2.5 μM hemin.
319 Incubation of cells in higher hemin concentrations did not allow to increase further β -Gal
320 activity.

321

322 **5. Heme incorporation in *L. sakei* is rapid and massive**

323 The absolute number of heme molecules incorporated by *L. sakei* 23K was also quantified
324 using ^{57}Fe -hemin (Fig. 5B). Cells were grown in MCD in the presence of labeled-hemin.
325 Measurements of the ^{57}Fe content of cells showed that the incorporation of ^{57}Fe -Hemin is

326 massive and rapid as bacteria are able to incorporate about 35,000 ^{57}Fe atoms of hemic
327 origin, within 1 hour in the presence of 1 μM ^{57}Fe -Hemin (Fig. 5B). The iron content of cells
328 increased to 160,000 and 260,000 atoms in average when bacteria were grown in a medium
329 containing 5 and 40 μM of ^{57}Fe -Hemin, respectively. This indicates that the ^{57}Fe content of *L.*
330 *sakei* cells increased with the ^{57}Fe -Hemin concentration in the medium on the 1 to 40 μM
331 range. Measurements of the iron content of bacteria, growing in presence of ^{57}Fe -Hemin for an
332 extended period of time (19h), did not show additional ^{57}Fe accumulation in the bacteria (Fig.
333 5B). Instead, the number of ^{57}Fe atoms associated with bacteria decreased over time,
334 highlighting the fact that a massive incorporation of labeled-hemin occurs rapidly after bacteria
335 being in contact with the molecules.

336

337 **Discussion**

338 Heme acquisition systems are poorly documented in lactic acid bacteria, probably because
339 heme or iron are not mandatory for growth of these bacterial species, at least under non-aerobic
340 conditions. However, acquisition of exogenous heme allows numerous lactic acid bacteria,
341 among them *L. lactis* and *Lactobacillus plantarum*, to activate, if needed, a respiratory
342 metabolism, when grown in the presence of oxygen (2, 49, 50). This implies that heme has to
343 cross the thick cell-wall of these Gram-positive organisms and may require heme transporters.
344 Thus far, heme acquisition systems in heme auxotrophic organisms have only been reported for
345 *Streptococci* (20, 21) and *S. pyogenes*, where they both involve Shr and Shp NEAT-domain
346 proteins and Hts ABC transporter (20, 22, 23). To our knowledge, in lactic acid bacteria, NEAT
347 domains have been identified in several species of lactic acid bacteria, including 15
348 *Lactobacillus*, 4 *Leuconostoc* and one *Carnobacterium* species (19) but no such functional
349 heme transport has been identified so far and our present study confirmed that *L. sakei* proteins
350 are devoid of such domains.

351 In *L. lactis*, the *fhuCBGDR* operon has been reported to be involved in heme uptake as a *fhuD*
352 mutant is defective in respiration metabolism, suggesting a defect in heme import (15). A
353 genome analysis of several lactic acid bacteria has revealed that a HupC/FepC heme uptake
354 protein is present in *L. lactis*, *L. plantarum*, *Lactobacillus brevis* and *L. sakei* (15). This latter in
355 *L. sakei* 23K may correspond to locus *lsa0399* included in a *fhu* operon. An IsdE homolog has
356 also been reported in *L. brevis* genome but the identity of this protein has not been
357 experimentally verified (15).

358 The genome analysis of *L. sakei* 23K (13), when focused on heme/iron transport systems and
359 heme utilization enzymes, led to the identification of several putative iron transport systems,
360 heme transport systems and heme-degrading enzymes. This heme uptake potential is
361 completely consistent within the meat environment-adapted *L. sakei*. Similarly, the membrane
362 transport system encoded by the *lsa1194-1195* genes, whose function is poorly defined, seems
363 to be important for the bacterial physiology as a *lsa1194-1195* deletion affects the survival
364 properties of this strain (see Supplemental text, Fig. S3 and Fig. S4).

365 Meanwhile, here, we report that the transcriptional unit *lsa1836-1840* shows exquisite
366 structure/function homology with the cobalamin ECF transporter, a new class of ATP-binding
367 cassette importer recently identified in the internalization of cobalt and nickel ions (Fig. 2 and
368 Fig. 3). Indeed, a comprehensive bioinformatics analysis indicates that the *lsa1836-1840* locus
369 codes for 5 proteins that assemble together to describe a complete importer machinery called
370 Energy Coupling Factor. Any canonical ECF transporter comprises an energy-coupling module
371 consisting of a transmembrane T protein (EcfT), two nucleotide-binding proteins (EcfA and
372 EcfA'), and another transmembrane substrate-specific binding S protein (Ecsf). Indeed,
373 Lsa1836-Lsa1838 shows high structural homology with Ecf-S, EcfA-A' and Ecf-T,
374 respectively. Despite sharing similarities with ABC-transporters, ECF transporters have
375 different organizational and functional properties. The lack of soluble-binding proteins in ECF

376 transporters differentiates them clearly from the canonical ABC-importers. Nevertheless here,
377 *lsa1839* and *lsa1840* code for proteins structurally close to β and α subunits of transcobalamin-
378 binding domain, respectively. They are highly suspected to be soluble proteins dedicated to
379 scavenge heme from the extracellular compartment, and we hypothesize that they could bind it
380 and then transfer it to Ecf-S component coded by *lsa1836* (Fig. 3). In line with that, the
381 heterodimer composed of Lsa1839 & Lsa1840, possibly β and α subunits, respectively, has
382 been modeled *in silico* and was shown to accommodate, with high affinity, an iron-heme ligand
383 at the binding site, located at the interface of the two proteins.

384 Internalization of the cobalt and nickel divalent cations through porphyrin moiety *via* this new
385 class of importer has been demonstrated in lactic acid bacteria, such as *L. lactis* and *L. brevis*.
386 However, nothing was known for the internalization/incorporation of iron-containing heme. A
387 functional analysis of the *lsa1836-1840* gene products was undertaken using Δ *lsa1836-1840*
388 deletion mutant and a complemented strain. Our experiments indicate that the intracellular
389 abundance of heme is significantly reduced in Δ *lsa1836-1840* mutant bacterial cells at 1 and 5
390 μ M heme, while it is similar to the WT at low heme concentrations. Reversely, the mutant
391 strain, in which *lsa1836-1840* is expressed from a multicopy plasmid, showed an increase in
392 the heme uptake. Taken together, these experiments confirm that the Lsa1836-1840 system is
393 involved *in vitro* in the active incorporation of heme in *L. sakei*. To our knowledge, this is the
394 first time that an ECF is reported to being involved in heme incorporation. One could consider
395 that such an ability to transport and accumulate heme/iron may represent an ecological fitness
396 trait for surviving in the heme-rich meat ecosystem, where heme does not represent a limiting
397 resource that would lead for competition strategies between species. This is probably true, not
398 only for *L. sakei* but also for the other meat resident species as our synteny analysis for this
399 operon shows that this feature could be shared within several Gram-positive meat-borne
400 bacteria.

401 Additionally, we were able to quantify the amount of heme internalized in the three genetic
402 contexts using isotope-labeled hemin and ICP-MS as well as to evaluate the intracellular
403 content of heme using the transcriptional fusion tool. We observed that the intracellular
404 abundance of heme increases with the concentration of heme in the growth medium and can be
405 detected with the intracellular sensor in the 0 - 2.5 μM heme range (Fig. 5A). The drop in the β -
406 gal activity at higher heme concentrations may result from regulation of heme/iron homeostasis
407 either through exportation of heme, degradation of the intracellular heme or storage of the
408 heme molecules, making them unable to interact with HrtR and promoting *lacZ* repression.
409 However, data obtained with the intracellular sensor at higher heme concentration (5-40 μM)
410 contrast with microscopic observations (Fig. S2) and ICP-MS measurements (Fig. 5B), that
411 reported a higher hemic-iron content in cells grown in 40 μM heme than in 5 μM . Indeed, β -
412 gal activity reflecting the abundance of intracellular heme was maximal when cells were grown
413 in a medium containing 1-2.5 μM hemin (Fig. 5A), while ICP-MS measurements showed a 4.5
414 fold and 8 fold higher number of ^{57}Fe atoms in bacteria growing in 5 μM or 40 μM ^{57}Fe -Hemin,
415 respectively, than in 1 μM ^{57}Fe -Hemin (Fig. 4B). These data are in good agreement with EELS
416 analysis (Fig. S2), which strengthens the hypothesis that heme homeostasis occurs in *L. sakei*
417 and that the incorporated heme molecules would be degraded while iron is stored inside iron
418 storage proteins like Dps, of which orthologous genes exist in *L. sakei*. Thus, iron is detected in
419 *L. sakei* cells but not bound to heme and unable to interact with the intracellular heme sensor
420 HrtR. Storage of heme inside membrane proteins is still an open question as *L. sakei* does not
421 contain cytochromes nor menaquinones (12).
422 Further analysis is required not only to decipher the exact role of these proteins during the
423 different steps of heme transport across the *L. sakei* membrane and the fate of heme inside *L.*
424 *sakei* cells, but also to understand the molecular specificity of the Lsa1836-1840 machinery
425 towards iron-containing heme *versus* cobalamin.

426

427 **Materials and methods**

428

429 **Bacterial strains and general growth conditions.**

430 The different bacterial strains used throughout this study are described in Table 1.

431 *Lactobacillus sakei* and its derivatives (RV2002 hrtR-lac RV4056 RV4056c RV4057

432 RV4057 hrtR-lac) were propagated on MRS (2) at 30°C. For physiological studies, the

433 chemically defined medium MCD (3) supplemented with 0.5% (wt/vol) glucose was used.

434 MCD contains no iron sources but contains possible traces of iron coming from various

435 components or distilled water. Incubation was performed at 30°C without stirring. Cell growth

436 and viability of cells in stationary phase were followed by measuring the optical density at 600

437 nm (OD₆₀₀) on a visible spectrophotometer (Secoman) and by the determination of the number438 of CFU ml⁻¹ after plating serial dilutions of samples on MRS agar. When needed, media were439 supplemented with filtered hemin or hematin (Sigma-Aldrich) or with ⁵⁷Fe-hemin (Frontier

440 Scientific) solutions resuspended in 50 mM NaOH.

441 *Escherichia coli* K-12 strain DH5 α was used as the host for plasmid construction and cloning442 experiments. *E. coli* cells were chemically transformed as previously described (4). *L. sakei*443 cells were transformed by electroporation as previously described (5). For routine growth, *E.*444 *coli* strain was propagated in LB at 37°C under vigorous shaking (175 rpm). The following445 concentrations of antibiotic were used for bacterial selection: kanamycin at 20 μ g/mL and446 ampicillin at 100 μ g/mL for *E. coli* and erythromycin at 5 μ g/mL for *L. sakei*.

447

448 **DNA manipulations.**

449 Chromosomal DNA was extracted from Ls cells with DNA Isolation Kit for Cells and Tissues

450 (Roche, France). Plasmid DNA was extracted from *E. coli* by a standard alkaline lysis

451 procedure with NucleoSpin[®] Plasmid Kit (Macherey Nagel, France). PCR-amplified fragments
452 and digested fragments separated on 0.8% agarose gels were purified with kits from Qiagen
453 (France). Restriction enzymes, *Taq* or *Phusion* high-fidelity polymerase (ThermoScientific,
454 France) and T4 DNA ligase (Roche) were used in accordance with the manufacturer's
455 recommendations. Oligonucleotides (Table 3) were synthesized by Eurogentec (Belgium).
456 PCRs were performed in Applied Biosystems 2720 Thermak thermocycler (ABI). Nucleotide
457 sequences of all constructs were determined by MWG - Eurofins (Germany).

458

459 **Bioinformatic analyses**

460 Analyses were performed in the sequenced *L. sakei* 23K genome (accession number:
461 CR936503) as described in (13). Each fasta sequence of every gene of the operon comprised
462 between *lsa1836* and *lsa1840* was retrieved from UniProtKB server at
463 <http://www.uniprot.org/uniprot>, uploaded then analyzed using HHpred server (44) that detects
464 structural homologues. For Lsa1839 and Lsa1840, that partly shares strong structural homology
465 with Geranyl-geranyltransferase type-I (pdb id 5nsa, chain A) (51), and β domain of human
466 haptocorrin (pdb id 4kki chain A) (52), intrinsic factor with cobalamin (pdb id 2pmv) (53) and
467 transcobalamin (pdb id 2bb6 chainA) (54) respectively, homology modeling was performed
468 using Modeler, version Mod9v18 (55). The heterodimer was then formed with respect to the
469 functional and structural assembly of α and β domains of the native haptocorrin (52). Upon
470 dimer formation, the best poses for heme inside the groove, which is located at the interface of
471 this heterodimer, were computed using Autodock4 tool (56). The protocol and grid box were
472 previously validated with the redocking of cyanocobalamin within human haptocorrin (4kki)
473 (42) and of cobalamin within bovine transcobalamin (2bb6). To compute the binding energy of
474 every complex, the parameters of the cobalt present in the cobalamin and cyanocobalamin were
475 added to the parameter data table, whilst the iron parameters of the heme were already noted in

476 the parameter data table. Then the docking poses were explored using the Lamarckian genetic
477 algorithm, and were subsequently analyzed with PyMOL of the Schrödinger suite (57).

478 Comparative genomic analysis for conservation of gene synteny between meat-borne bacteria
479 was carried out with the MicroScope Genome Annotation platform, using the Genome
480 Synteny graphical output and the PkGDB Synteny Statistics (58)

481

482 **Construction of plasmids and *L. sakei* mutant strains.**

483 All the primers and plasmids used in this study are listed in Table 2 and 3. The *lsa1836-1840*
484 genes were inactivated by a 5118 bp deletion using double cross-over strategy. Upstream and
485 downstream fragments were obtained using primers pairs PHDU-*lsa1836F*/PHDU-*lsa1836R*
486 (731 bp) and PHDU-*lsa1840F*/PHDU-*lsa1840R* (742 bp) (Table 3). PCR fragments were joined
487 by SOE using primers PHDU-*lsa1836F*/PHDU-*lsa1840R*, and the resulting 1456 bp fragment
488 was cloned between *EcoRI* and *KpnII* sites in pRV300 yielding the pRV441 (Table 2). pRV441
489 was introduced in the *L. sakei* 23K and the *L. sakei* 23K $\Delta lacLM$ (RV2002) strains by
490 electroporation as described previously (59). Selection was done on erythromycin sensitivity.
491 Second cross-over erythromycin sensitive candidates were screened using primers PHDU-
492 *crb1sa1840F* and PHDU-*crb1sa1840R* (Table 3). Deletion was then confirmed by sequencing
493 the concerned region and the *lsa1836-1840* mutant strains were named RV4056 and RV4057
494 (Table 2).

495 To construct the RV2002 *hrtR-lac* and the RV4057 *hrtR-lac* strains, the pP_{hrt}*hrtR-lac* (Table 2)
496 was transformed by electroporation into the corresponding mother strains.

497 For complementation, a pP_{lsa1836-1840} plasmid (Table 2) was constructed as follows: a DNA
498 fragment encompassing the promoter and the 5 genes of the *lsa1836-1840* operon was PCR
499 amplified, using the primers pair *Lsa1836R/Lsa1840F* (Table 3). The 5793 bp amplified
500 fragment was cloned into plasmid pRV566 at *XmaI* and *NotI* sites. The construct was verified

501 by sequencing the whole DNA insert using the 566-F and 566-R primers (Table 3) as well as
502 internal primers. The *pPlsa1836-1840* was introduced into RV4056 bacteria by electroporation
503 and transformed bacteria were selected for erythromycin resistance, yielding the RV4056c
504 complemented mutant strain.

505

506 **β -galactosidase assay**

507 Liquid cultures were usually grown in MCD into exponentially phase corresponding to a A_{600}
508 equal to 0,5-0.8 and then incubated for 1 h at 30°C with hemin at the indicated concentration.
509 β -Galactosidase (β -Gal) activity was assayed on bacteria permeabilized as described. β -Gal
510 activity was quantified by luminescence in an Infinite M200 spectroluminometer (Tecan), using
511 the β -Glo® assay system as recommended by manufacturer (Promega).

512

513 **Intracellular iron ^{57}Fe determination**

514 The various strains were grown in MCD to $A_{600} = 0.5-0.7$ at 30°C, prior to addition or not of
515 0.1, 1, 5 or 40 μM ^{57}Fe -labelled hemin (Frontier Scientific). Cells were then incubated at 30°C
516 for an additional hour and overnight (19 hours). Cells were washed three times in H_2O
517 supplemented with 1mM EDTA. Cell pellets were desiccated and mineralized by successive
518 incubations in 65% nitric acid solution at 130°C. ^{57}Fe was quantified by Inductively Coupled
519 Plasma Mass Spectroscopy (ICP-MS) (Agilent 7700X), Géosciences, University of Montpellier
520 (France).

521

522 **Statistical analysis**

523 To determine if the differences in heme incorporation by *L. sakei* cells grown in the presence of
524 increasing concentrations of heme, measured using the molecular reporter, were different from
525 the control condition (cells grown in the absence of heme), the non-parametrical Kruskal-

526 Wallis followed by the Dunn's multiple comparisons test with a family-wise significance and a
527 confidence level of 0.05 was performed using GraphPad Prism version 8.4.2 for macOS,
528 GraphPad Software, La Jolla California USA, www.graphpad.com.

529

530 **Acknowledgments**

531 This work, including Emilie Verplaetse post-doctoral grant, was funded from the French
532 National Research Agency ANR-11-IDEX-0003-02; 'ALIAS' project.

533 The authors would like to thank Véronique Martin for her help in setting up the cobalt
534 parameter in the Autodock table parameter, Elise Abi-Khalil for the construction of the
535 pLsa1836-1840, Delphine Lechardeur and Alexandra Gruss for the heme reporter plasmid and
536 fruitful discussion and support.

537

538

539 **References**

- 540 1. Neilands JB. 1981. Microbial Iron Compounds. *Annu Rev Biochem* 50:715–731.
- 541 2. Brooijmans R, Smit B, Santos F, van Riel J, de Vos WM, Hugenholtz J. 2009. Heme
542 and menaquinone induced electron transport in lactic acid bacteria. *Microb Cell Factories* 8:28.
- 543 3. Pandey A, Bringel F, Meyer J-M. 1994. Iron requirement and search for siderophores in
544 lactic acid bacteria. *Appl Microbiol Biotechnol* 40:735–739.
- 545 4. Zagorec M, Champomier-Vergès M-C. 2017. *Lactobacillus sakei*: A Starter for Sausage
546 Fermentation, a Protective Culture for Meat Products. *Microorganisms* 5:56.
- 547 5. Bredholt S, Nesbakken T, Holck A. 1999. Protective cultures inhibit growth of *Listeria*
548 *monocytogenes* and *Escherichia coli* O157:H7 in cooked, sliced, vacuum- and gas-packaged
549 meat. *Int J Food Microbiol* 53:43–52.
- 550 6. Leroy F, Lievens K, De Vuyst L. 2005. Modeling Bacteriocin Resistance and
551 Inactivation of *Listeria innocua* LMG 13568 by *Lactobacillus sakei* CTC 494 under Sausage
552 Fermentation Conditions. *Appl Environ Microbiol* 71:7567–7570.
- 553 7. Vermeiren L, Devlieghere F, Debevere J. 2004. Evaluation of meat born lactic acid
554 bacteria as protective cultures for the biopreservation of cooked meat products. *Int J Food*
555 *Microbiol* 96:149–164.
- 556 8. Chaillou S, Christeans S, Rivollier M, Lucquin I, Champomier-Vergès MC, Zagorec
557 M. 2014. Quantification and efficiency of *Lactobacillus sakei* strain mixtures used as protective
558 cultures in ground beef. *Meat Sci* 97:332–338.
- 559 9. Devlieghere F, Francois K, Vereecken KM, Geeraerd AH, Van Impe JF, Debevere J.
560 2004. Effect of chemicals on the microbial evolution in foods. *J Food Prot* 67:1977–1990.
- 561 10. Lombardi-Boccia G, Martinez-Dominguez B, Aguzzi A. 2002. Total Heme and Non-
562 heme Iron in Raw and Cooked Meats. *J Food Sci* 67:1738–1741.
- 563 11. Hertel C, Schmidt G, Fischer M, Oellers K, Hammes WP. 1998. Oxygen-Dependent

- 564 Regulation of the Expression of the Catalase Gene *katA* of *Lactobacillus sakei* LTH677. Appl
565 Environ Microbiol 64:1359–1365.
- 566 12. Duhutrel P, Bordat C, Wu T-D, Zagorec M, Guerquin-Kern J-L, Champomier-Verges
567 M-C. 2010. Iron Sources Used by the Nonpathogenic Lactic Acid Bacterium *Lactobacillus*
568 *sakei* as Revealed by Electron Energy Loss Spectroscopy and Secondary-Ion Mass
569 Spectrometry. Appl Environ Microbiol 76:560–565.
- 570 13. Chaillou S, Champomier-Vergès M-C, Cornet M, Crutz-Le Coq A-M, Dudez A-M,
571 Martin V, Beaufils S, Darbon-Rongère E, Bossy R, Loux V, Zagorec M. 2005. The complete
572 genome sequence of the meat-borne lactic acid bacterium *Lactobacillus sakei* 23K. Nat
573 Biotechnol 23:1527–1533.
- 574 14. Huang W, Wilks A. 2017. Extracellular Heme Uptake and the Challenge of Bacterial
575 Cell Membranes. Annu Rev Biochem 86:799–823.
- 576 15. Gruss A, Borezée-Durant E, Lechardeur D. 2012. Chapter Three - Environmental Heme
577 Utilization by Heme-Auxotrophic Bacteria, p. 69–124. In Robert K. Poole (ed.), Advances in
578 Microbial Physiology. Academic Press.
- 579 16. Choby JE, Skaar EP. 2016. Heme Synthesis and Acquisition in Bacterial Pathogens. J
580 Mol Biol 428:3408–3428.
- 581 17. Anzaldi LL, Skaar EP. 2010. Overcoming the Heme Paradox: Heme Toxicity and
582 Tolerance in Bacterial Pathogens. Infect Immun 78:4977–4989.
- 583 18. Reniere ML, Torres VJ, Skaar EP. 2007. Intracellular metalloporphyrin metabolism in
584 *Staphylococcus aureus*. BioMetals 20:333–345.
- 585 19. Honsa ES, Maresso AW, Highlander SK. 2014. Molecular and Evolutionary Analysis of
586 NEAr-Iron Transporter (NEAT) Domains. PLoS ONE 9:e104794.
- 587 20. Bates CS, Montanez GE, Woods CR, Vincent RM, Eichenbaum Z. 2003. Identification
588 and Characterization of a *Streptococcus pyogenes* Operon Involved in Binding of

- 589 Hemoproteins and Acquisition of Iron. *Infect Immun* 71:1042–1055.
- 590 21. Meehan M, Burke FM, Macken S, Owen P. 2010. Characterization of the haem-uptake
591 system of the equine pathogen *Streptococcus equi subsp. equi*. *Microbiology* 156:1824–1835.
- 592 22. Lei B, Smoot LM, Menning HM, Voyich JM, Kala SV, Deleo FR, Reid SD, Musser
593 JM. 2002. Identification and Characterization of a Novel Heme-Associated Cell Surface
594 Protein Made by *Streptococcus pyogenes*. *Infect Immun* 70:4494–4500.
- 595 23. Ouattara M, Bentley Cunha E, Li X, Huang Y-S, Dixon D, Eichenbaum Z. 2010. Shr of
596 group A *Streptococcus* is a new type of composite NEAT protein involved in sequestering
597 haem from methaemoglobin: Haem uptake and reduction by Shr. *Mol Microbiol* 78:739–756.
- 598 24. Lechardeur D, Cesselin B, Liebl U, Vos MH, Fernandez A, Brun C, Gruss A, Gaudu P.
599 2012. Discovery of Intracellular Heme-binding Protein HrtR, Which Controls Heme Efflux by
600 the Conserved HrtB-HrtA Transporter in *Lactococcus lactis*. *J Biol Chem* 287:4752–4758.
- 601 25. Joubert L, Derré-Bobillot A, Gaudu P, Gruss A, Lechardeur D. 2014. HrtBA and
602 menaquinones control haem homeostasis in *Lactococcus lactis*: Membrane and intracellular
603 haem control in *Lactococcus lactis*. *Mol Microbiol* 93:823–833.
- 604 26. Rempel S, Stanek WK, Slotboom DJ. 2019. ECF-Type ATP-Binding Cassette
605 Transporters. *Annu Rev Biochem* 88:551–576.
- 606 27. Finkenwirth F, Eitinger T. 2019. ECF-type ABC transporters for uptake of vitamins and
607 transition metal ions into prokaryotic cells. *Res Microbiol*.
- 608 28. Wang T, Fu G, Pan X, Wu J, Gong X, Wang J, Shi Y. 2013. Structure of a bacterial
609 energy-coupling factor transporter. *Nature* 497:272–276.
- 610 29. Bao Z, Qi X, Hong S, Xu K, He F, Zhang M, Chen J, Chao D, Zhao W, Li D, Wang J,
611 Zhang P. 2017. Structure and mechanism of a group-I cobalt energy coupling factor transporter.
612 *Cell Res* 27:675–687.
- 613 30. Zhang M, Bao Z, Zhao Q, Guo H, Xu K, Wang C, Zhang P. 2014. Structure of a

- 614 pantothenate transporter and implications for ECF module sharing and energy coupling of
615 group II ECF transporters. Proc Natl Acad Sci U S A 111:18560–18565.
- 616 31. Xu K, Zhang M, Zhao Q, Yu F, Guo H, Wang C, He F, Ding J, Zhang P. 2013. Crystal
617 structure of a folate energy-coupling factor transporter from *Lactobacillus brevis*. Nature
618 497:268–271.
- 619 32. Rodionov DA, Hebbeln P, Eudes A, ter Beek J, Rodionova IA, Erkens GB, Slotboom
620 DJ, Gelfand MS, Osterman AL, Hanson AD, Eitinger T. 2009. A novel class of modular
621 transporters for vitamins in prokaryotes. J Bacteriol 191:42–51.
- 622 33. Henderson GB, Zevely EM, Huennekens FM. 1979. Mechanism of folate transport in
623 *Lactobacillus casei*: evidence for a component shared with the thiamine and biotin transport
624 systems. J Bacteriol 137:1308–1314.
- 625 34. Burgess CM, Slotboom DJ, Geertsma ER, Duurkens RH, Poolman B, van Sinderen D.
626 2006. The riboflavin transporter RibU in *Lactococcus lactis*: molecular characterization of gene
627 expression and the transport mechanism. J Bacteriol 188:2752–2760.
- 628 35. Turner MS, Tan YP, Giffard PM. 2007. Inactivation of an Iron Transporter in
629 *Lactococcus lactis* Results in Resistance to Tellurite and Oxidative Stress. Appl Environ
630 Microbiol 73:6144–6149.
- 631 36. Li L, Chen OS, Ward DM, Kaplan J. 2001. CCC1 Is a Transporter That Mediates
632 Vacuolar Iron Storage in Yeast. J Biol Chem 276:29515–29519.
- 633 37. Fernandez A, Lechardeur D, Derré-Bobillot A, Couvé E, Gaudu P, Gruss A. 2010. Two
634 Coregulated Efflux Transporters Modulate Intracellular Heme and Protoporphyrin IX
635 Availability in *Streptococcus agalactiae*. PLoS Pathog 6:e1000860.
- 636 38. von Heijne G. 1992. Membrane protein structure prediction. Hydrophobicity analysis
637 and the positive-inside rule. J Mol Biol 225:487–494.
- 638 39. Jin B, Newton SMC, Shao Y, Jiang X, Charbit A, Klebba PE. 2006. Iron acquisition

- 639 systems for ferric hydroxamates, haemin and haemoglobin in *Listeria monocytogenes*. Mol
640 Microbiol 59:1185–1198.
- 641 40. Abi-Khalil E, Segond D, Terpstra T, Andre-Leroux G, Kallassy M, Lereclus D, Bou-
642 Abdallah F, Nielsen-Leroux C. 2015. Heme interplay between IIsA and IsdC: Two structurally
643 different surface proteins from *Bacillus cereus*. Biochim Biophys Acta 1850:1930–1941.
- 644 41. Maresso AW, Chapa TJ, Schneewind O. 2006. Surface Protein IsdC and Sortase B Are
645 Required for Heme-Iron Scavenging of *Bacillus anthracis*. J Bacteriol 188:8145–8152.
- 646 42. Mazmanian SK, Skaar EP, Gaspar AH, Humayun M, Gornicki P, Jelenska J, Joachmiak
647 A, Missiakas DM, Schneewind O. 2003. Passage of heme-iron across the envelope of
648 *Staphylococcus aureus*. Science 299:906–909.
- 649 43. Mazmanian SK, Ton-That H, Su K, Schneewind O. 2002. An iron-regulated sortase
650 anchors a class of surface protein during *Staphylococcus aureus* pathogenesis. Proc Natl Acad
651 Sci 99:2293–2298.
- 652 44. Söding J, Biegert A, Lupas AN. 2005. The HHpred interactive server for protein
653 homology detection and structure prediction. Nucleic Acids Res 33:W244–248.
- 654 45. Szklarczyk D, Gable AL, Lyon D, Junge A, Wyder S, Huerta-Cepas J, Simonovic M,
655 Doncheva NT, Morris JH, Bork P, Jensen LJ, Mering C von. 2019. STRING v11: protein–
656 protein association networks with increased coverage, supporting functional discovery in
657 genome-wide experimental datasets. Nucleic Acids Res 47:D607–D613.
- 658 46. Roberts JN, Singh R, Grigg JC, Murphy MEP, Bugg TDH, Eltis LD. 2011.
659 Characterization of Dye-Decolorizing Peroxidases from *Rhodococcus jostii* RHA1.
660 Biochemistry 50:5108–5119.
- 661 47. Singh R, Grigg JC, Armstrong Z, Murphy MEP, Eltis LD. 2012. Distal Heme Pocket
662 Residues of B-type Dye-decolorizing Peroxidase: arginine but not aspartate is essential for
663 peroxidase activity. J Biol Chem 287:10623–10630.

- 664 48. Lauret R, Morel-Deville F, Berthier F, Champomier-Verges M, Postma P, Ehrlich SD,
665 Zagorec M. 1996. Carbohydrate utilization in *Lactobacillus sake*. *Appl Environ Microbiol*
666 62:1922–1927.
- 667 49. Gaudu P, Vido K, Cesselin B, Kulakauskas S, Tremblay J, Rezaiki L, Lamberret G,
668 Sourice S, Duwat P, Gruss A. 2002. Respiration capacity and consequences in *Lactococcus*
669 *lactis*. *Antonie Van Leeuwenhoek* 82:263–269.
- 670 50. Lechardeur D, Cesselin B, Fernandez A, Lamberet G, Garrigues C, Pedersen M, Gaudu
671 P, Gruss A. 2011. Using heme as an energy boost for lactic acid bacteria. *Curr Opin Biotechnol*
672 22:143–149.
- 673 51. Bloch JS, Ruetz M, Kräutler B, Locher KP. 2017. Structure of the human
674 transcobalamin beta domain in four distinct states. *PLOS ONE* 12:e0184932.
- 675 52. Furger E, Frei DC, Schibli R, Fischer E, Prota AE. 2013. Structural Basis for Universal
676 Corrinoid Recognition by the Cobalamin Transport Protein Haptocorrin. *J Biol Chem*
677 288:25466–25476.
- 678 53. Mathews FS, Gordon MM, Chen Z, Rajashankar KR, Ealick SE, Alpers DH, Sukumar
679 N. 2007. Crystal structure of human intrinsic factor: Cobalamin complex at 2.6-Å resolution.
680 *Proc Natl Acad Sci* 104:17311–17316.
- 681 54. Wuerges J, Garau G, Geremia S, Fedosov SN, Petersen TE, Randaccio L. 2006.
682 Structural basis for mammalian vitamin B12 transport by transcobalamin. *Proc Natl Acad Sci*
683 103:4386–4391.
- 684 55. Webb B, Sali A. 2016. Comparative Protein Structure Modeling Using MODELLER.
685 *Curr Protoc Bioinforma* 54:5.6.1-5.6.37.
- 686 56. Morris GM, Goodsell DS, Halliday RS, Huey R, Hart WE, Belew RK, Olson AJ. 1998.
687 Automated docking using a Lamarckian genetic algorithm and an empirical binding free energy
688 function. *J Comput Chem* 19:1639–1662.

- 689 57. The PyMOL Molecular Graphics System, Version 2.0. Schrödinger, LLC.
- 690 58. Vallenet D, Belda E, Calteau A, Cruveiller S, Engelen S, Lajus A, Le Fèvre F, Longin
691 C, Mornico D, Roche D, Rouy Z, Salvignol G, Scarpelli C, Thil Smith AA, Weiman M,
692 Médigue C. 2013. MicroScope—an integrated microbial resource for the curation and
693 comparative analysis of genomic and metabolic data. *Nucleic Acids Res* 41:D636–D647.
- 694 59. Berthier F, Zagorec M, Champomier-Verges M, Ehrlich SD, Morel-Deville F. 1996.
695 Efficient transformation of *Lactobacillus sake* by electroporation. *Microbiology* 142:1273–
696 1279.
- 697 60. Stentz R, Loizel C, Malleret C, Zagorec M. 2000. Development of Genetic Tools for
698 *Lactobacillus sakei*: Disruption of the β -Galactosidase Gene and Use of *lacZ* as a Reporter
699 Gene To Study Regulation of the Putative Copper ATPase, AtkB. *Appl Environ Microbiol*
700 66:4272–4278.
- 701 61. Leloup L, Ehrlich SD, Zagorec M, Morel-Deville F. 1997. Single-crossover integration
702 in the *Lactobacillus sake* chromosome and insertional inactivation of the *ptsI* and *lacL* genes.
703 *Appl Environ Microbiol* 63:2117–2123.
- 704 62. Alpert C-A, Crutz-Le Coq A-M, Malleret C, Zagorec M. 2003. Characterization of a
705 Theta-Type Plasmid from *Lactobacillus sakei*: a Potential Basis for Low-Copy-Number
706 Vectors in *Lactobacilli*. *Appl Environ Microbiol* 69:5574–5584.
- 707
708
709
710
711

712 **Table 1:** Genes putatively involved in iron/heme transport and heme modification

Locus tag and	Protein ID	Predicted protein function
Functional category		
Genes putatively involved in iron/heme transport		
ABC transporters		
<i>Isa0399-0402</i>	CAI54700-CAI54703	Fhu
<i>Isa1836-1840</i>	CAI56143-CAI56147	Putative metal ion ABC transporter, cobalamin transporter
<i>Isa1366-1367</i>	CAI55670-CAI55671	Putative ABC exporter (heme-efflux machinery)
Proton-motive force transporters		
<i>Isa0246</i>	CAI54546	Mn ²⁺ / Zn ²⁺ / Fe ²⁺ transporter
<i>Isa1699</i>	CAI56006	Mn ²⁺ / Zn ²⁺ / Fe ²⁺ transporter
Membrane proteins		
<i>Isa1194-1195</i>	CAI55498-CAI55499	Uncharacterized proteins
Gene putatively involved in heme modification		
<i>Isa1831</i>	CAI56138	Dyp-type peroxidase

713

714

715 **Table 2:** Strains and plasmids used in this study

716

Strains or plasmids	Characteristics	References
Strains		
<i>Lactobacillus sakei</i> 23K	sequenced strain	(13)
RV2002	23K derivative, $\Delta lacLM$	(60)
RV2002 hrtR-lac	RV2002 carrying the pP _{hrt} hrtR-lac, ery ^R	This study
RV4056	23K derivative, $\Delta isa1836-1840$	This study
RV4056c	RV4056 carrying the pP _{isa1836-1840} , ery ^R	This study
RV4057	RV2002 $\Delta isa1836-1840$	This study
RV4057 hrtR-lac	RV4057 carrying the pP _{hrt} hrtR-lac, ery ^R	This study
Plasmids		
pP _{hrt} hrtR-lac	Plasmid carrying the P _{hrt} hrtR-lac transcriptional fusion	(24)
pRV300	Shuttle vector, non-replicative in <i>Lactobacillus</i> ; Amp ^R , Erm ^R	(61)
pRV566	vector used for complementation; Amp ^R , Erm ^R	(62)
pRV441	pRV300 derivative, exchange cassette for <i>isa1836-1840</i>	This study
pP _{isa1836-1840}	pRV566 carrying the promoter and the <i>isa1836-1840</i> coding sequences	This study

717

718

719

720

721

722

723 **Table 3:** Oligonucleotides used in this study

Primer	Sequence ^a (5'-3')	Restriction site
PHDU- <i>lsa1836F</i>	CAT <u>GGTACC</u> GGTCGGCTCAATTATGAGT	<i>KpnI</i>
PHDU- <i>lsa1836R</i>	AATGAACTAGTTAGCGCTCGCAGCCTATATTGCGAGT	
PHDU- <i>lsa1840F</i>	AGCGCTAACTAGTTCATTAGACTTCCGTCACCTGTGAA	
PHDU- <i>lsa1840R</i>	CTGGAATTCATGCTGAGCGATGGTTTCT	<i>EcoRI</i>
PHDU- <i>crblsa1840F</i>	CGACAAGTCAACTCAGTGCTA	
PHDU- <i>crblsa1840R</i>	GTGAACCGTAATCTTGAGTG	
<i>Lsa1836R</i>	TT <u>CCCGGGA</u> ACTTACAAAAGGCCACGC	<i>XmaI</i>
<i>Lsa1840F</i>	AAAAG <u>CGGCCGCGC</u> CTCCTTATAAAAACTG	<i>NotI</i>
566-F	GCGAAAGAATGATGTGTTGG	
566-R	CACACAGGAAACAGCTATGAC	

724

725 ^a underlined sequences indicate the location of restriction sites, and italicized letters indicate

726 complementary overlapping sequences used to join PCR fragments as described in the

727 materials and methods section.

728

729 **Legends**

730

731 Figure 1: Gene synteny within and around the *lsa1836-1840* gene cluster of *L. sakei* 23K with
732 other Gram-positive species found frequently on meat products. Genes in grey background are
733 unrelated to this cluster and are not conserved between the different genomes. The name of the
734 species and of the strains used for analysis are depicted on the right. All of these species
735 contain a *katA* gene (encoding a heme-dependent catalase) in their genome. Other meat-borne
736 species including *Leuconostoc*, *Lactococcus*, *Vagococcus* species also found on meat are not
737 shown due to the lack of both *katA* gene and *lsa1836-1840* gene cluster.

738

739 Figure 2: Panel A details the structural and functional bioinformatic assessment for each gene
740 of the *lsa1836-1840* operon. Panel B focuses on Lsa1839 and Lsa1840 and highlights (left) the
741 binding interaction and affinity of the human haptocorrin with cyano-cobalamin and bovine
742 transcobalamin with cobalamin, respectively. They were used as 3D template and positive
743 control for the modeling of transcobalamin-like proteins Lsa1840 and Lsa1839. Panel B (right)
744 shows the best pose of iron containing heme as computed by Autodock4 within the binding
745 pocket formed at the interface of a and b subunits of homology modeled Lsa1840 and Lsa1839,
746 respectively. The polar and hydrophobic interactions between the heme and α plus β chains are
747 highlighted as brown sticks.

748

749 Figure 3: A, Functional reannotation of the operon *lsa1836-1840* from *L. sakei* 23K after serial
750 analysis of 3D structure/function prediction for each gene of the operon. B, Reconstitution of
751 iron-containing heme transport, initially scavenged between the a and b subunits of the
752 transcobalamine-like transporter, coded by *lsa1839-1840*, then cargoed from the extracellular
753 into the intracellular compartments through the complete ECF machinery coded by *lsa1836-*

754 1838 portion of the operon. Possibly, gene *lsa1831* positioned in the vicinity of the loci
755 *lsa1836-1840* could code for a protein Dyp-type peroxidase that ultimately releases the iron
756 from the heme.

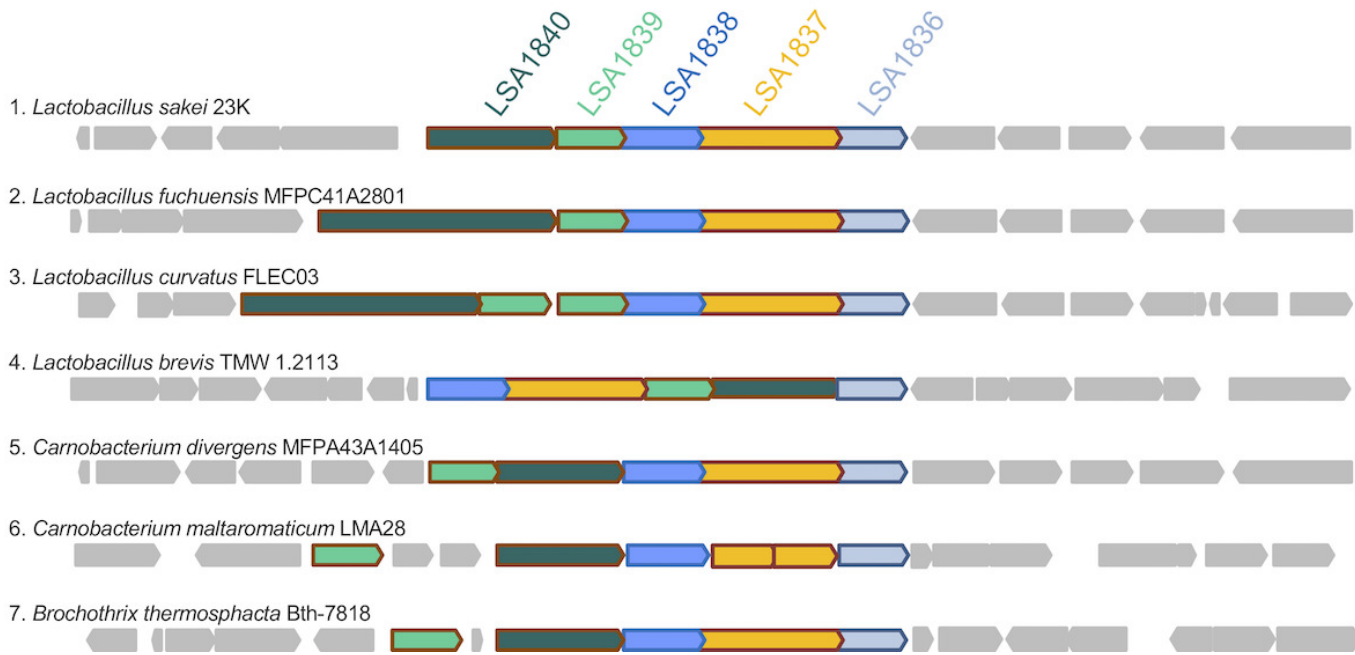
757

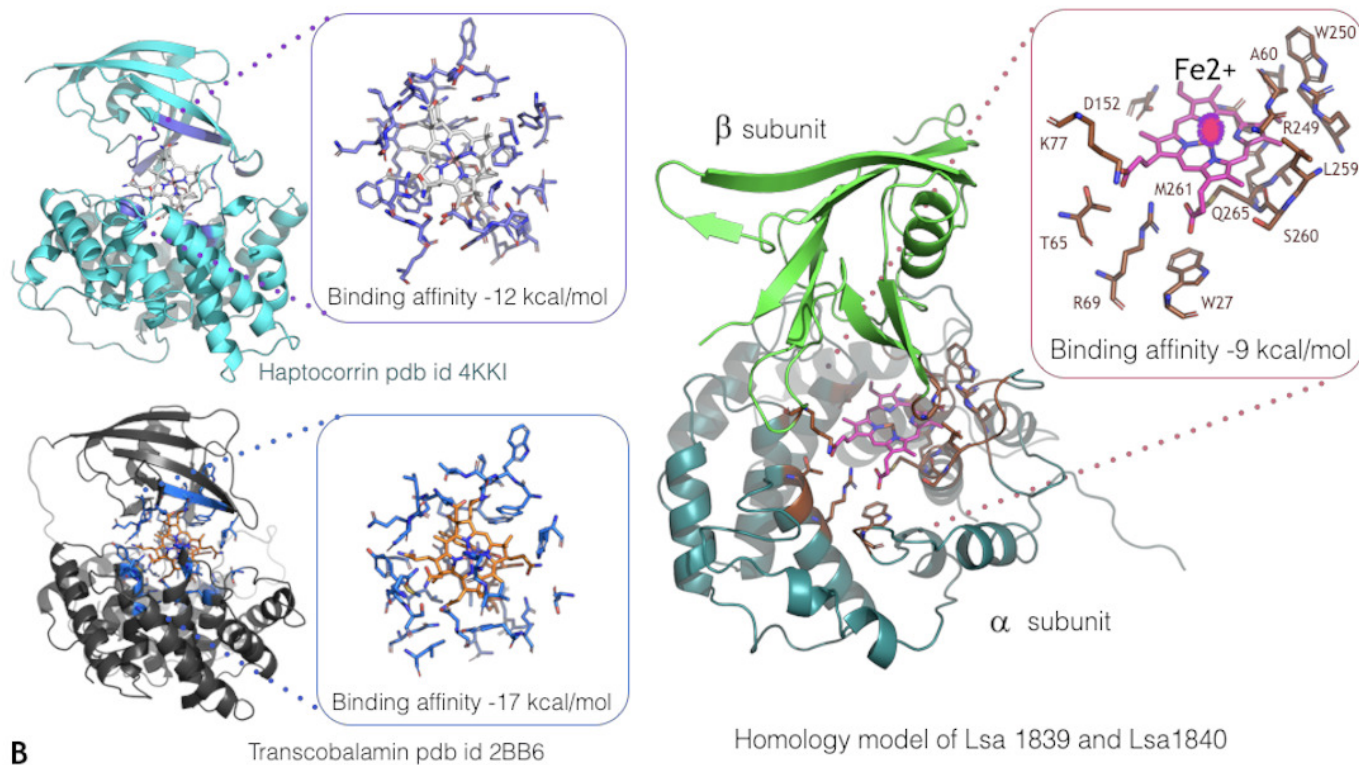
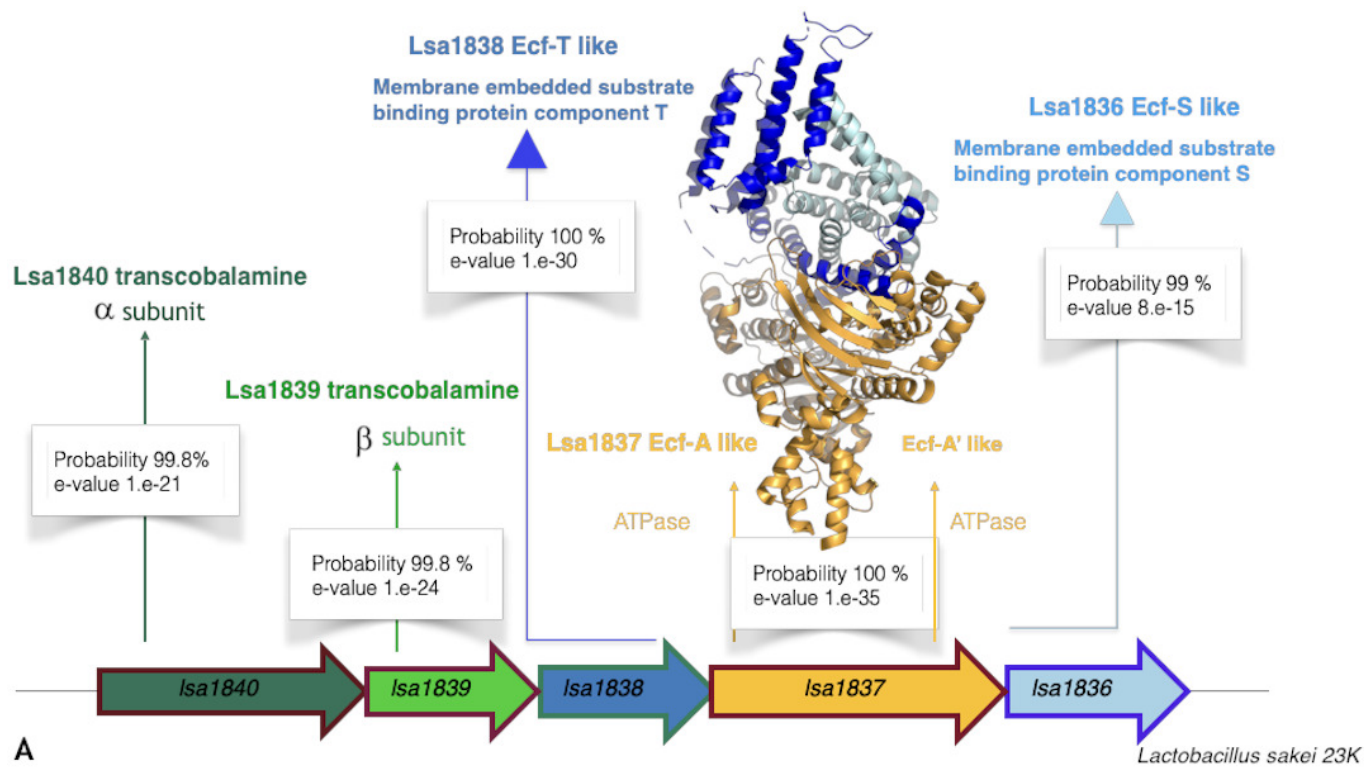
758 Figure 4: Heme incorporation is reduced in the Δ *lsa1836-1840* *L. sakei* deletion mutant. A, *In*
759 *vivo* detection of intracellular heme content of the RV2002 and Δ *lsa1836-1840* (RV4057)
760 mutant strains. Strains carrying the pP_{hrtR}*hrtR-lac* were grown in hemin and β -Gal activity was
761 quantified by luminescence (see “Materials and methods”). For each experiment, values of
762 luminescence obtained with no added hemin are subtracted and β -Gal activity of strains was
763 expressed as the percentage to the RV2002 strain for each hemin concentration. Mean values
764 are shown (n=3). Error bars represent the standard deviation. B, Quantification of the ⁵⁷Fe
765 content of the WT (23K) and the Δ *lsa1836-1840* (RV4056) strains grown in the absence and
766 presence of indicated ⁵⁷Fe-hemin concentrations. Results represent the mean and range from at
767 least two independent experiments. C, Quantification of the ⁵⁷Fe content of the WT (23K), the
768 Δ *lsa1836-1840* (RV4056) and the Δ *lsa1836-1840* pP_{lsa1836-1840} (RV4056c) strains grown in
769 the absence and presence of indicated ⁵⁷Fe-hemin concentrations. Results represent the mean
770 and range of two independent experiments.

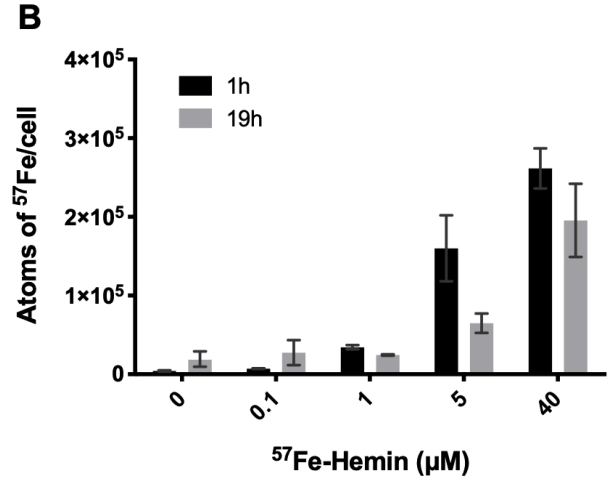
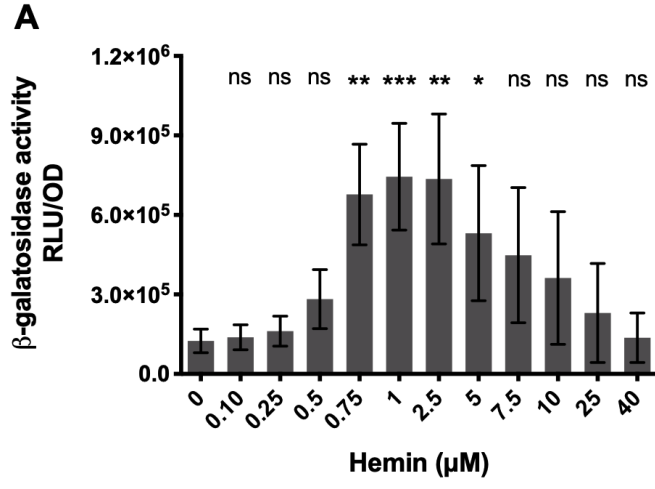
771

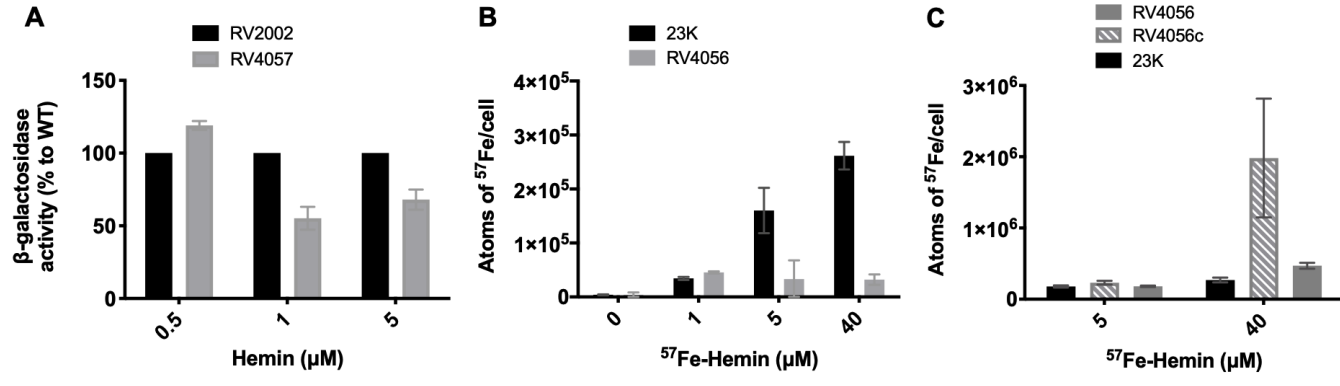
772 Figure 5: Quantification of heme incorporation in *L. sakei*. A, *In vivo* detection of intracellular
773 heme molecules through the expression of the *lacZ* gene. The *L. sakei* RV2002 *hrtR-lac* strain
774 was grown for 1 h in the presence of the indicated concentrations of hemin. β -Gal activity was
775 quantified by luminescence (see “Materials and methods”). Mean values are shown (n=7).
776 Error bars represent the standard deviation. Conditions for which the β -Gal activity of cells is
777 different as compared to the control condition (0 μ M Hemin) are indicated with stars.
778 Significance is based on Kruskal- Wallis followed by the Dunn’s multiple comparisons test

779 with a $P < 0.05^*$, $P < 0.01^{**}$, $P < 0.001^{***}$. B, Quantification of the ^{57}Fe content of the WT (23K)
780 strain grown in the absence and presence of ^{57}Fe -hemin for 1h and 19h. The mean values and
781 range of two independent experiments are shown. RLU, relative light units.

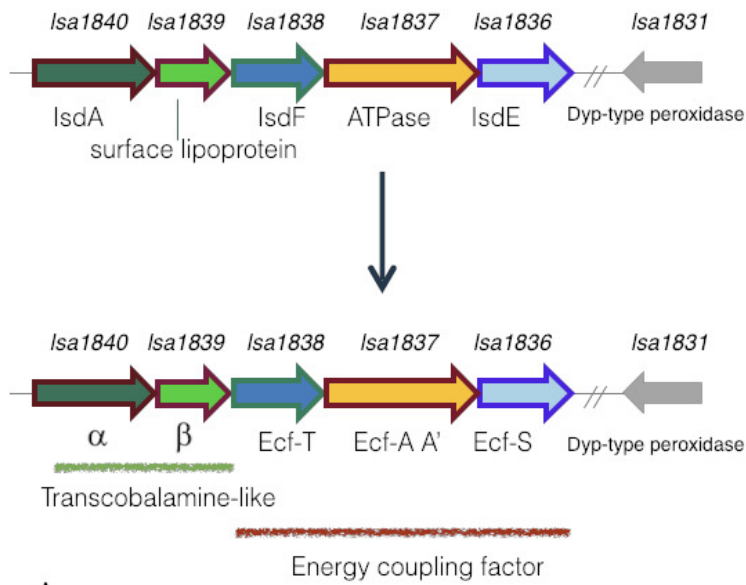








Functional reannotation of the operon



Heme cargoed from outside to inside

